

# PARTICLE VOLUME RECONSTRUCTION BASED ON A MARKED POINT PROCESS AND APPLICATION TO TOMO-PIV

*R. Ben Salah*<sup>1,2</sup>, *O. Alata*<sup>3</sup>, *B. Tremblais*<sup>2</sup>, *L. Thomas*<sup>1</sup>, *L. David*<sup>1</sup>

<sup>1</sup>University of Poitiers, Pprime Institute, Fluid, Thermic and Combustion Department, CNRS 3346

<sup>2</sup>University of Poitiers, Xlim Laboratory, SIC Department, CNRS 7252

<sup>3</sup>University Jean Monnet of Saint-Etienne, Hubert Curien Laboratory, CNRS 5516

{riadh.ben.salah, benoit.tremblais, lionel.thomas}@univ-poitiers.fr  
olivier.alata@univ-st-etienne.fr

## ABSTRACT

In this paper, we propose a new tomographic reconstruction method, called IOD-PVRMPP, to reconstruct 3D particle volumes from 2D particle images provided by the Tomographic Particle Image Velocimetry (Tomo-PIV) technique. Our method, based on marked point processes (or object processes), allows to solve the problem in a parsimonious way. It facilitates the introduction of prior knowledge and solves memory problem which is inherent to voxel based approaches used by classical tomographic reconstruction methods. The reconstruction of a 3D particle set is obtained by minimizing an energy function which defines the marked point process. To this aim, we use a simulated annealing algorithm based on Reversible Jump Markov Chain Monte Carlo (RJCMC) method. To speed up the convergence of the simulated annealing, we develop an initialization method which provides the initial distribution of 3D particles. To do that, we proceed by detecting 2D particles located in projection images. Using synthetic data, we show that IOD-PVRMPP method gives better results than MinLOS-MART method for different seeding densities.

**Index Terms**— Marked Point Processes or Object Processes, Tomography Reconstruction, Simulated Annealing, RJCMC, Tomo-PIV.

## 1. INTRODUCTION

Tomographic reconstruction techniques appeared in 1970 and have been firstly used in the medical field. With the development of the Tomo-PIV by Elsinga et al [1], algebraic reconstruction techniques (ART) have been extended to the PIV field to reconstruct distributions of 3D particles in order to study complex flows. Tomo-PIV is based on a multi-sensor recording. It consists in measuring instantaneously the three velocity components of a flow from the displacement of the tracer particles recorded using several cameras from different viewing angles. Tomographic reconstruction methods are well suited to resolve the problem of limitation in number of views, but they are very expensive in computation time and memory storage.

Many researches in Tomo-PIV field focused on tomographic reconstruction techniques to solve the problem of computation time. For this purpose, a study conducted by Worth and Nickels [2] yielded

an approach named MFG (Multiplicative First Guess) for fast object reconstruction. Atkinson and Soria [3] developed the MinLOS-MART method to accelerate MART method (Multiplicative ART) which is the most used algebraic technique in Tomo-PIV field [4]. Another technique to accelerate computation time is MG (multi-grid) method conducted by Discetti and Astarita [5]. It consists in reconstructing discretized objects with a low resolution. After identifying regions with active voxels, these regions are updated with high resolution. Petra et al [6] investigated the mathematical properties of tomographic reconstruction on synthetic data. They work on theoretical foundations for particle volume's sparse representation and showed that applying parsimonious reconstruction algorithms in this context gives better results than classical-state-of-the-art methods such as algebraic reconstruction. On 2012, Wieneke [7] proposed an algorithm called IPR (Iterative Particle Reconstruction) to reconstruct 3D-particle locations by comparing the recorded images with generated ones calculated from the particle distribution in the volume. Particles in the reconstructed volume are represented by 3D-positions instead of voxel-based intensity blobs as in MART. Recently, Schanz et al [8] proposed a method called Shake The Box (STB) to track 3D particle positions. STB method produces a prediction of the particle distribution of already tracked particles and refines the found positions by an image-matching scheme. This predicted particle distribution is used as an initialization to the IPR process to reduce iteration number.

Nevertheless, already proposed tomographic reconstruction techniques does not sufficiently take into account the particular shape of objects to be reconstructed. Given the size of data, the processing time of the methods and the memory usage are still very high. To solve these problems, a solution based on the parsimony of particle volumes can be considered. Thus, a method to reconstruct 3D particle volumes based on an "object" processes seems particularly well suited [9]. Stochastic models based on marked point processes (or object processes) have been used in various application fields such as detection of tree crowns [10], populations of birds [11], or road networks [9]. These models have proved their efficiency for object extraction in large sample spaces.

This paper focuses on the reconstruction of 3D particle volumes in large configuration spaces, formulated in marked point process reconstruction framework. We then finalize a previous work [12] by proposing an efficient initialization method and running simulations until realistic particle densities. It is organized as follows: in section 2, after some recalls on marked point processes, we provide the new method, called IOD-PVRMPP (Initialization by Object Detection

---

The current work has been conducted as part of the AFDAR project, Advanced Flow Diagnostics for Aeronautical research, funded by the European Commission program FP7, grant n°265695 and the FEDER project n°34754

- Particle Volume Reconstruction based on Marked Point Process) and how to simulate it. In section 3, we compare IOD-PVRMPP to MinLOS-MART using synthetic data with different seeding densities. The focus will be on the quality of the reconstructed volumes. In section 4, we conclude the paper and give some prospects for the work.

## 2. PARTICLE VOLUME RECONSTRUCTION BASED ON MARKED POINT PROCESS

### 2.1. Basics of marked point processes

In this section, we recall the basic ideas of PP (point processes) and MPP (marked PP) [13, 14]. An MPP can be called an “object” process (OP) when the mark define a geometric object [9] as in our case: the objects are the particles. In the following, we will use OP for 2D particles and MPP for 3D particles.

Let  $K \subset \mathbb{R}^3$  be an observation domain with volume  $0 < \nu(K) < \infty$ . A PP on  $K$  is a finite configuration of points  $\{k_i \in K, i = 1, \dots, N\}$  such as  $k_i \neq k_j$  for  $i \neq j$ . To form more complex objects, we can attach characteristics or marks to the points. Let  $(M, \mathcal{M}, \nu_M)$  the probability space which describes the marks. A finite random configuration of marked points (or objects) is a sample of a MPP only if the position process of objects is a PP. Based on this definition, volume or image features are viewed as a set of objects identified jointly by their positions in the image and their geometrical characteristics. For a more complete presentation of MPP, the reader is referred to [9, 15].

Our aim is to reconstruct a set of particles (2D or 3D) based on the light energy acquired in the projections (images). Unlike classic tomographic reconstruction methods, the objective is to obtain particles that belong to a continuous space (*i.e.* a position of a  $n$ D particle belongs to  $\mathbb{R}^n$ ,  $n = 2$  or  $3$ ). Following the elements previously recalled, points represent center positions of  $n$ D particles and marks provide center intensities, forms and radiuses. Thus, such configuration of  $n$ D particles is given by  $y = \{(k_1, m_1), \dots, (k_{n(y)}, m_{n(y)})\}$ .  $k_i \in K$  and  $m_i \in M$ ,  $i = 1, \dots, n(y)$ , represent the  $n$ D particle positions and the particle marks respectively. This process provides a naturally sparse representation of configurations of objects of interest located in a volume. They allow in fact detaching from the numerical model induced by the volume, constituted of voxels, to better approximate the physical model.

A configuration of an OP or a MPP is classically viewed as a sample issued from an unnormalized probability density  $f$  which is a Gibbs distribution:

$$f(y|\theta) \propto \exp(-U(y|\theta)) \quad (1)$$

with  $y$  a finite configuration of  $n$ D particles,  $\theta$  a set of fixed parameters. The energy  $U(y|\theta)$  allows us to model interactions between particles and it's composed of the sum of two terms: 1) a data driven energy denoted  $U_d(y|\theta_d)$  that reflects the adequacy between configurations of  $n$ D particles and the observed data and 2) an internal energy denoted  $U_{\text{int}}(y|\theta_{\text{int}})$  that reflects an *a priori* on such configurations. This leads to the following expression:

$$U(y|\theta) = U_d(y|\theta_d) + U_{\text{int}}(y|\theta_{\text{int}}) \quad (2)$$

and  $\theta = \theta_d \cup \theta_{\text{int}}$ . Thus, for a given value of  $\theta$  parameters, the most likely configuration (with total energy equal to the global minimum) allows the particle volume reconstruction:

$$\hat{y} = \underset{y}{\operatorname{argmax}} f(y|\theta) = \underset{y}{\operatorname{argmin}} U(y|\theta) \quad (3)$$

The computation of the global minimum of the energy is performed by a simulated annealing which is a stochastic method of optimization [16, 17]. This technique is based on the simulation of a non-homogeneous Markov Chain (see [9, 18] for example and section 3 for implementation details).

An appropriate definition of the data energy allows us to obtain marked points (particles) that are consistent with respect to a given observation. In our case, this energy will enable the process to converge to an appropriate configuration of  $n$ D particles.

### 2.2. Initialization method based on object detection

In tomographic reconstruction field and specially in fluid mechanics field where data size and particle density are very high, the initialization process is a very important step that can speed up the convergence of the reconstruction methods and enhance the reconstruction quality. To compute a first estimation of the reconstructed volume, we propose an “Object Oriented” method called IOD (Initialization by Object Detection) which was inspired from a 3D position reconstruction technique named “triangulation” often used in computer vision field. This initialization procedure represents the main contribution of this paper and will be used before PVRMPP method [12], whose aim is to obtain a 3D particle set. Let us notice that IOD can also be used with any other tomographic reconstruction method applied to Tomo-PIV. The operating mode of this 3D particle volume initialization method is applied to  $P$  acquired projection images and can be realized in 3 main steps: 1) detection of 2D particles in each projection image; 2) identification of epipolar 2D particles; 3) reconstruction of 3D particles from 2D epipolar particles marks.

#### 2.2.1. 1<sup>st</sup> step: 2D particles detection

To detect 2D particles in the projection images, we modify the 3D particles reconstruction algorithm based on MPP, proposed in [12], in 2D subspace. Like 3D particles, a 2D particle is characterized by its intensity distribution, its size and its isotropic or anisotropic Gaussian-shape. The data driven energy is derived from the mean square error (MSE) between an image generated from a population of 2D particles  $y_i = \{\zeta_{i,j}\}_{j=1, \dots, n(y_i)}$  and corresponding acquired image  $I_i$ ,  $i = 1, \dots, P$ :

$$MSE(y_i, I_i) = \sum_{s \in I_i} (o_{i,s} - p_{i,s})^2 \quad (4)$$

where  $o_{i,s}$  is the observed value on pixel  $s$  of image  $I_i$  and  $p_{i,s}$  the generated value by the 2D particles configuration  $y_i$  on pixel  $s$ . If we develop  $MSE$  expression with the deletion of constant terms we can obtain the expression of a data driven energy as a sum of two energies  $U_{d,1}(y_i|\theta_d) + U_{d,2}(y_i|\theta_d)$  defined as follows:

$$\begin{aligned} U_{d,1}(y_i|\theta_d) &= \sum_{\zeta_{i,j} \in y_i} \phi_{d,1}(\zeta_{i,j}) \\ U_{d,2}(y_i|\theta_d) &= \sum_{\zeta_{i,j} \sim \zeta_{i,k}} \phi_{d,2}(\zeta_{i,j}, \zeta_{i,k}) \end{aligned} \quad (5)$$

where

$$\begin{aligned} \phi_{d,1}(\zeta_{i,j}) &= \sum_{s \in I_i, \zeta_{i,j} \rightarrow s} p_{\zeta_{i,j} \rightarrow s} (p_{\zeta_{i,j} \rightarrow s} - 2 o_{i,s}) \\ \phi_{d,2}(\zeta_{i,j}, \zeta_{i,k}) &= \sum_{s \in I_i} 2 p_{\zeta_{i,j} \rightarrow s} p_{\zeta_{i,k} \rightarrow s} \end{aligned} \quad (6)$$

As the Gaussian spatial extension of the intensity of an object is truncated (see Sec. 3),  $\zeta_{i,j} \rightarrow s$  means that  $\zeta_{i,j}$  contains  $s \in I_i$

and  $p_{\zeta_{i,j} \rightarrow s}$  represents the intensity value generated on  $s$  by  $\zeta_{i,j}$ . When two particles contains the same pixel  $s$ , they are considered as neighbors:  $\zeta_{i,j} \sim \zeta_{i,k}$  if  $\exists s \in I_i$  s.t.  $p_{\zeta_{i,j} \rightarrow s}$  and  $p_{\zeta_{i,k} \rightarrow s}$ . The behavior of this data driven energy is quite similar to the one used for 3D particle volume reconstruction model [12] where  $\phi_{d,1}$  acts like a correlation operator between a particle and the values at its position in acquired image and  $\phi_{d,2}$  penalizes particles which have same position in acquired image.

In the proposed model, the internal energy is divided in a sum of two terms and can be written as follows:

$$U_{\text{int}}(y_i|\theta_{\text{int}}) = U_e(y_i|\theta_e) + U_s(y_i|\theta_s) \quad (7)$$

The first term  $U_e(y_i|\theta_e) = -n(y_i) \log(\beta)$  is an energy associated with the PP intensity in terms of number of particles  $n(y_i)$  inside a configuration. It is defined by  $\beta$  intensity parameter. The second term  $U_s(y_i|\theta_s) = -n_a(y_i) \log(\gamma_a)$  allows defining a Strauss point process which belongs to the family of Marked point processes [13, 18]. When  $0 \leq \gamma_a < 1$ , this component penalizes aggregation of 2D particles.  $n_a(y_i)$  represents the number of neighbor relationships between 2D particles in the following sense:  $\zeta_{i,j} \overset{S}{\sim} \zeta_{i,k}$  if  $\|k_{i,j} - k_{i,k}\|_2 \leq r_{i,j} + r_{i,k}$  where  $r_{i,j}$  and  $r_{i,k}$  are the radiuses of  $\zeta_{i,j}$  and  $\zeta_{i,k}$  respectively. The value of hyper-parameter  $\gamma_a \in [0, 1]$  controls the outcome of the potential function. If  $\gamma_a = 1$ , the process defined by  $U_{\text{int}}$  behaves as an homogeneous Poisson PP with intensity  $\beta$ . If  $\gamma_a \in ]0, 1[$ , pairs of 2D particles with distance less than  $r_{i,j} + r_{i,k}$  are penalized. If  $\gamma_a = 0$ , the process forbids that two points exist within distance  $r_{i,j} + r_{i,k}$ . The process is then said to be hard core. Let us notice that  $\gamma_a$  should be chosen near 0 for a 3D process (the particles are solid then there exists theoretically no spatial intersection) and near 1 for a 2D process (superpositions can occur for the projections of the particles).

The proposed model is then parameterized by  $\theta = \theta_d \cup \theta_{\text{int}}$  with  $\theta_{\text{int}} = \{\beta, \gamma_a\}$ .  $\theta_d$  is mainly defined by 2D particle model (minimum and maximum values for their intensities and radiuses).

To limit the number of iterations and speed up the convergence of the simulated annealing, we develop a simple initialization procedure, called IRW (Iterative Random Walk), in order to propose a first distribution of 2D particles. To this aim, one iteration of this procedure is performed on 3 steps: a simple peak detection is applied to the image which gives a set of detected 2D positions ; each position of this set will be transformed to a 2D particle by moving the corresponding position randomly in order to enhance its data driven energy ; a residual image which will be used in the next iteration, is computed between the image used for peak detection and the generated one from 2D particle set. In section 3, the number of iterations is fixed equal to two.

### 2.2.2. 2<sup>nd</sup> step: epipolar 2D particles identification

Once the detection of 2D particles is completed, we apply a search algorithm to identify epipolar 2D particles. In our case, a set of  $P$  2D particles, which belong to their respective projections, are considered epipolars if they are located inside  $P$  2D Boxes obtained by the projection of a unique 3D box.

This step is carried out by decomposing the volume on 3D box subspaces by following the principle of Octree structure. We start with a 1<sup>st</sup> level decomposition. Each 3D Box is projected to give  $P$  epipolar 2D Boxes. A search for 2D particles inside each obtained 2D Box is then performed. If a set of 2D epipolar particles is found, a reconstruction procedure is realized to create an associated 3D particle inside the corresponding 3D Box. The level of Octree decomposition increases if one 2D Box contains more than one 2D particle.

### 2.2.3. 3<sup>rd</sup> step: 3D particles reconstruction

The reconstruction quality of 3D particles is highly dependent to robustness of 2D particle detection algorithm of IOD method. The aim of this final step of IOD method is to compute the marks of each 3D particle which contains the intensity distribution and size (radius). They are computed by back-projecting the  $P$  epipolar 2D particles marks. Positions of 3D particles can be obtained by back-projecting 2D particles coordinates for known  $z$  values which represent positions on line of sight. In our case, searching for  $z$  value based on positions of epipolar 2D particles represents a minimization problem that consists on minimizing distance between back-projection of each 2D particle and their centroid.

## 2.3. Simulation of Marked Point Processes

PP and MPP (or OP) are classically simulated using RJMCMC exploiting a Metropolis-Hasting-Green (MHG) dynamic [9, 19]. This dynamic allows to simulate a process with varying sampling spaces. In our case, these sampling spaces are associated with configurations with different numbers of particles. The basic moves of RJMCMC for MPP are birth and death moves [13, 20].

In addition to these moves, a configuration can be changed by moving positions of objects. To obtain a better position, an object inside the configuration is randomly chosen and new positions are randomly sampled using a uniform probability inside a spherical area around the original position. The proposed position is the one that gives the minimal value of data driven energies.

Then, the proposed state for a population of  $n$ D particles  $y$ , is  $y' = y \cup \{\xi\}$  for the birth case, where  $\xi$  is a randomly proposed particle. For the death move, the proposed state is  $y' = y \setminus \{\xi\}$ , where  $\xi$  is chosen inside  $y$ . For the translation move, the proposed state can then be written as  $y' = y \setminus \{\xi_1\} \cup \{\xi_2\}$  where  $\xi_1$  is a chosen object inside  $y$  and  $\xi_2$  is a proposed particle randomly chosen near  $\xi_1$ .

The different propositions are accepted with probability  $\min\{1, \tau_i\}$ ,  $i = B, D$  or  $TR$  (for Birth, Death and Translation), with  $\tau_i$  the MHG acceptance ratio. For each move,  $\tau_i$  is proportional (see [9] for complete formulas) to the ratio  $\frac{f(y'|\theta)}{f(y|\theta)} = \exp\{-\Delta U\}$ ,  $\Delta U = U(y'|\theta) - U(y|\theta)$ , where  $y'$  is the proposed configuration. As we have defined a Markov object process,  $\Delta U$  will only depend on  $\xi$  and its neighbors [12]. Thus, it can be efficiently computed.

A simulated annealing can be realized by dividing  $U_d + U_s$  by a temperature  $T$  and simulating the modified process from a high temperature  $T_0$  to a low temperature  $T_f$ . The complete algorithm (called IOD-PVRMPP) contains the two following steps: 1) IOD method that provides a set of 2D detected particles for each projection,  $i = 1, \dots, P$  and the initial 3D particle set computed from the 2D particle set; 2) PVRMPP method that provides the final 3D particle configuration (see [12] for more details).

We provide now some experimental results.

## 3. RESULTS

A set of synthetic volumes with associated projected images have been generated using an image generator developed in C++ using the SLIP library [21]. The synthetic volume size is  $500 \times 500 \times 150$ . Four projections of size  $500 \times 500$ , with image seeding density varying from 0.0004 to 0.2 ppp (particle per pixel), are then computed knowing that 0.05 ppp is the reference seeding density level for Tomo-PIV field [1]. 2D and 3D particles are characterized by

marks as described in section 2 and [12]. The number of 3D particles  $N_p$  in synthetic volumes, generated for each seeding density level, are varying from 100 up to 50000 particles. 1570104905

ppp	$N_p$	$\beta$	$T_0$	$f_b$	$f_{tr}$	$N_{it}$
0.0004	100	$2.66 \cdot 10^{-6}$	0.025	0.50	0.50	$15 \cdot 10^3$
0.0008	200	$5.33 \cdot 10^{-6}$	0.025	0.50	0.50	$18 \cdot 10^3$
0.0020	500	$1.33 \cdot 10^{-5}$	0.035	0.50	0.50	$24 \cdot 10^3$
0.0040	1000	$2.66 \cdot 10^{-5}$	0.045	0.50	0.50	$50 \cdot 10^3$
0.0080	2000	$5.33 \cdot 10^{-5}$	0.045	0.50	0.50	$13 \cdot 10^4$
0.0200	5000	$1.33 \cdot 10^{-4}$	0.048	0.60	0.50	$55 \cdot 10^4$
0.0500	12500	$3.33 \cdot 10^{-4}$	0.850	0.75	0.40	$81 \cdot 10^5$
0.1000	25000	$6.66 \cdot 10^{-4}$	0.850	0.75	0.40	$25 \cdot 10^6$
0.2000	50000	$1.33 \cdot 10^{-3}$	0.850	0.75	0.40	$32 \cdot 10^6$

**Table 1.** Sets of parameters used for PVRMPP experiments.

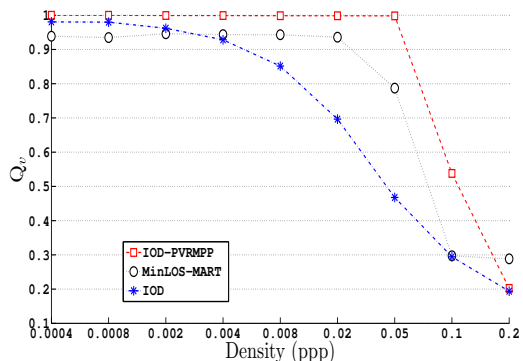


**Fig. 1.** Evolution of the volume reconstruction quality  $Q_v$  against density of particles.

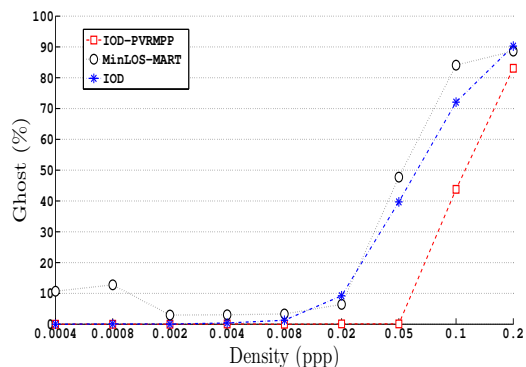


**Fig. 2.** Evolution of percentage of number of ghost particles against density of particles

For this experimental study, we fixed the intensity center and the radius of all particles: the diameter size is  $5 \times 5 \times 5$  voxels for 3D particles and  $3 \times 3$  pixels for 2D particles; the distribution of intensities around all center positions of particles is modeled as a multivariate isotropic Gaussian density. The calibration model is a pinhole model, without distortions. The acquisition system is simulated with 4 cameras ( $P = 4$ ): two cameras on one side with a  $30^\circ$  viewing angle; two other cameras on the other side of the volume, in a same plane [4]. For PVRMPP, a set of parameters (see Sec. 2) has been chosen for each seeding density in order to get a good reconstruction of 3D particle volumes (see table 1). These choices of parameters were adopted after several simulations, trying to find the best trade-off between reconstruction quality, ghost

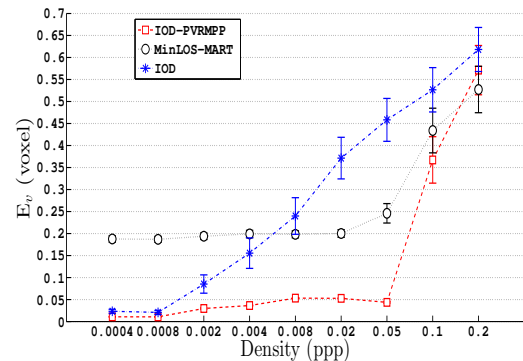


**Fig. 3.** Evolution of error position in volume against density of particles.

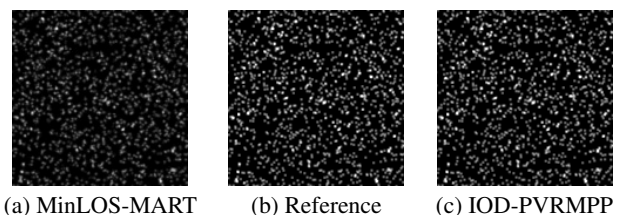


**Fig. 4.** Comparison of the projections of a reconstructed particles volume onto a camera for (a) MinLOS-MART, (b) Reference (c) IOD-PVRMPP for 0.05 ppp seeding density level.

particles rate and computation time with regard to optimized MART method's robustness. In table 1,  $f_{tr}$  corresponds to the probability of selecting the translation move. Birth and death moves are chosen with the probability  $1 - f_{tr}$ , and, in a second random selection, with the probabilities  $f_b$  and  $f_d$  respectively ( $f_d = 1 - f_b$ ).  $\gamma_a$  is fixed to 0.05. The simulated annealing algorithm is configured with an initial temperature  $T_0$  and with a fixed final temperature  $T_f$  equal to 0.02. A classical cooling scheme has been chosen:  $T_t = T_0 q^t$  with  $t$  the current iteration,  $q = \left(\frac{T_f}{T_0}\right)^{\frac{1}{N_{it}}}$  the parameter of the cooling scheme and  $N_{it}$  the number of iterations. Each iteration consists in one proposed "Birth"/"Death"/"Translation" move of RJMCMC dynamics, which may be accepted or not.

To evaluate the performances of IOD-PVRMPP method, we computed some quantitative measures and we compared them to those obtained with an optimized MinLOS-MART algorithm [4], with fixed number of iterations equal to two, which can be considered as a reference algorithm within our application. We also give the results of IOD method to show the improvement obtained between initial and final populations of points. All measures are computed by taking 10 reconstructed samples (volumes) for IOD-PVRMPP method given the random nature of the algorithm.

To evaluate the reconstruction quality, we have computed the cross-correlations ( $Q_v$ ) between the reconstructed volumes and the reference ones. Figure 1 shows that IOD-PVRMPP provides better results than MinLOS-MART for seeding densities up to 0.1 ppp. The reconstruction quality of IOD-PVRMPP method decreases when the overlapping between 2D particles in images increases.

To evaluate the accuracy of IOD-PVRMPP method, we computed error positions ( $E_v$ ) between 3D particle positions in reconstructed volumes and the reference. Results show a very high level of accuracy with error average varying between 0.01 to 0.043 voxel for

seeding density up to 0.05 ppp (Fig.3). Curves in (Fig.2) show very low rates of detected ghost particles with IOD-PVRMPP method which vary between 0 and 0.098% for seeding density up to 0.05 ppp against 2.92 to 47.74% with MinLOS-MART method. Some samples of projections after volume reconstruction are presented on (Fig.4) in order to provide some qualitative visual results.

In our experiments, computation times of IOD-PVRMPP, which needs considerably more iterations to converge without IOD, and MinLOS-MART are quite similar up to 0.02 ppp. Then it increases by increasing the seeding density level in images. But it should be noted that our algorithm is under development and further computation optimizations can still be done. Representation of particles via marks takes up very little space comparing to representation inside a 3D array volume: If just 8 parameter values are typically associated to a particle, particle distributions can be stored in less memory RAM than classical voxel storage. IOD-PVRMPP algorithm needs between 0.07 and 36 MB storage for these synthetic cases against 192 MB for MART algorithm. Gain in memory storage increases by increasing the size of the volume.

#### 4. CONCLUSION

In this paper, a new method for 3D particle volume reconstruction, including initialization procedure, using marked point process framework is presented. Rather than pixel-oriented or voxel-oriented, our work uses object-oriented approach. Optimization is done with a simulated annealing method using a RJMCMC dynamic. We have shown, on synthetic cases, the relevance of the proposed initialization procedure for the reconstruction of a 3D particle volume. The method is compared to MinLOS-MART. IOD-PVRMPP shows better results than MinLOS-MART for seeding densities up to 0.05 ppp. Future works will include the definition of new moves in the RJMCMC dynamic in order to change the radius and the center intensity of each particle. The method will be tested on noisy synthetic case and compare to other non voxel based techniques like IPR [7, 22]. It will be also applied to real experimental case to study its capacity to reconstruct 3D velocity fields.

#### REFERENCES

- [1] Elsinga G. E., Scarano F., and Wieneke B., "Tomographic particle image velocimetry," *Exp Fluids*, vol. 41, pp. 933–947, 2006.
- [2] Worth N. A. and Nickels T. B., "Acceleration of tomo-piv by estimating the initial volume intensity distribution," *Experiments in Fluids*, vol. 45, no. 5, pp. 847–856, 2008.
- [3] Atkinson C. H. and Soria J., "An efficient simultaneous reconstruction technique for tomographic particle image velocimetry," *Experiments in Fluids*, vol. 47, no. 4-5, pp. 553–568, 2009.
- [4] Thomas L., Tremblais B., and David L., "Optimization of the volume reconstruction for classical tomo-piv algorithms (mart, bimart and smart): synthetic and experimental studies," *Measurement Science and Technology*, vol. 25, no. 3, pp. 035303, 2014.
- [5] Discetti S. and Astarita T., "A fast multi-resolution approach to tomographic piv," *Experiments in Fluids*, vol. 52, no. 3, pp. 765–777, 2012.
- [6] Petra S., Schröder A., and Schnörr C., "3d tomography from few projections in experimental fluid dynamics," in *Imaging Measurement Methods for Flow Analysis*, vol. 106 of *Notes on Numerical Fluid Mechanics and Multidisciplinary Design*, pp. 63–72. Springer Berlin Heidelberg, 2009.
- [7] Wieneke B., "Iterative reconstruction of volumetric particle distribution," *Measurement Science and Technology*, vol. 24, no. 2, pp. 024008, 2013.
- [8] Schanz D., Schroder A., Gesemann S., Michaelis D., and Wieneke B., "'shake the box': A highly efficient and accurate tomographic particle tracking velocimetry (tomo-ptv) method using prediction of particle positions," in *PIV13*, 2013.
- [9] Stoica R., Descombes X., and Zerubia J., "A gibbs point process for road extraction from remotely sensed images," *Int. J. Computer Vision*, vol. 57, no. 2, pp. 121–136, May 2004.
- [10] Perrin G., Descombes X., and Zerubia J., "Adaptive simulated annealing for energy minimization problem in a marked point process application," in *Energy Minimization Methods in Computer Vision and Pattern Recognition*, vol. 3757 of *LNCIS*, pp. 3–17. Springer Berlin Heidelberg, 2005.
- [11] Descamps S., Descombes X., Bechet A., and Zerubia J., "Automatic flamingo detection using a multiple birth and death process," in *IEEE ICASSP 2008*, 2008, pp. 1113–1116.
- [12] Ben-Salah R., Alata O., Thomas L., Tremblais B., and David L., "3d particle volume tomographic reconstruction based on marked point process: Application to tomo-piv in fluid mechanics," in *IEEE ICASSP 2014*, 2014.
- [13] Van Lieshout M. N. M., *Markov point processes and their applications*, Imperial College Press/World Scientific Publishing,, 2000.
- [14] Daley D. J. and Vere-Jones D., *An Introduction to the Theory of Point Processes: Volume I: Elementary Theory and Methods, Second Edition*, vol. 1, Springer, New York, 2nd edn. springer edition, 2003.
- [15] Chatelain F., Costard A., and Michel O.J.J., "A bayesian marked point process for object detection. application to muse hyperspectral data," in *IEEE ICASSP 2011*, 2011, pp. 3628–3631.
- [16] Geman S. and Geman D., "Stochastic relaxation:gibbs distributions and the bayesian restoration of images," *IEEE Trans. on PAMI*, vol. 9, pp. 721–741, 1984.
- [17] Azencott R., *Simulated annealing: Parallelization techniques*, Springer-Verlag, NY, 1992.
- [18] Alata O., Burg S., and Dupas A., "Grouping/degrouping point process, a point process driven by geometrical and topological properties of a partition in regions," *Computer Vision and Image Understanding*, vol. 115, pp. 1324–1339, 2011.
- [19] Green P. J., "Reversible jump markov chain monte carlo computation and bayesian model determination," *Biometrika*, vol. 82, no. 4, pp. 711–732, 1995.
- [20] Preston C. J., "Spatial birth-and-death processes," *Bulletin of the International Statistical Institute*, vol. 46, pp. 371–391, 1977.
- [21] Tremblais B., David L., Arrivault D., Dombre J., Chatellier L., and Thomas L., "Slip : Simple library for image processing (version 1.0)," <http://sliplib.free.fr>, 2010.
- [22] Champagnat F., Cornic P., Cheminet A., Leclaire B., Le-Besnerais G., and Plyer A., "Tomographic piv: particles versus blobs," *Measurement Science and Technology*, vol. 25, no. 8, pp. 084002, 2014.